

Effects of Gd₂O₃ on structure and magnetic properties of Ni-Mn ferrite

LIJUN ZHAO, HUA YANG*, LIANXIANG YU, YUMING CUI

*College of Chemistry, Jilin University, Changchun, 130023, People's Republic of China**E-mail: huayang86@sina.com*

SHOUHUA FENG

*College of Chemistry, Jilin University, Changchun, 130023, People's Republic of China; State Key Laboratory of Inorganic Synthesis and Preparative Chemistry, Jilin University, Changchun, 130023, People's Republic of China***Published online:** 17 January 2006

The emulsion method was used to prepare nanocrystalline Ni_{0.7}Mn_{0.3}Gd_xFe_{2-x}O₄ ferrites. The growth of particles, the structure and the magnetic properties were investigated by X-ray diffraction (XRD), Mössbauer spectroscopy and vibrating sample magnetometer (VSM). Furthermore, the influence of Gd₂O₃ on magnetic properties of Ni-Mn ferrite powders has been investigated in detail. When the crystallite sizes are about 30–40 nm, all the samples have the similar Ms values. The variational rules of saturation magnetization (Ms) and coercivity (Hc) along with doped-Gd contents at different sintering temperatures show that the maximum Gd ions content doped into ferrite lattices is $x = 0.06$. When Gd-doped content x is larger than 0.06, the doped Gd ions can't enter into the ferrite lattice totally but reside at grain boundary, as the ionic radii of the Gd³⁺ ions are larger than that of Fe³⁺ ions. The ferrimagnetism have not disappeared completely, even if the crystallite size is 7.8 nm.

© 2006 Springer Science + Business Media, Inc.

1. Introduction

Ferrites, i.e. ferromagnetic cubic spinels possess the combined properties of magnetic materials and insulators. During last few decades, they have been studied extensively because of their importance in basic as well as in applied research [1]. The spinel ferrites (MFe₂O₄, M = a divalent cation) belong to an important class of magnetic materials because of their remarkable magnetic properties particularly in the radio frequency region, physical flexibility, high electrical resistivity, mechanical hardness, and chemical stability [2]. The magnetic properties of ferrites can be changed by the substitution of various kinds of M²⁺ among divalent cations (Zn²⁺, Mg²⁺, Cu²⁺, Mn²⁺, Ni²⁺, Co²⁺, Fe²⁺...), or by introducing a relatively small amount of rare-earth ions. In our experiment, the structural and magnetic properties of Ni-Mn ferrite doped with Gd₂O₃ were investigated. The particle size was varied by changed the duration of heat treatment above crystallization temperature.

2. Experimental

Nanocrystalline Ni_{0.7}Mn_{0.3}Gd_xFe_{2-x}O₄ ferrites were prepared by the emulsion method, using analytically pure grade Ni(NO₃)₂·6H₂O, Fe(NO₃)₃·9H₂O, Mn(NO₃)₂ and Gd₂O₃ as starting materials. PEG (molecular weight 20000) was used as the surfactant. The amount of the nitrates were mixed with PEG to form solution, then NH₄OH with the concentration of 2 M was dropped into the solution until PH = 9.5 to form the precipitate. The precipitate was washed with distilled water for three times and dried at 90 °C for 7 h to prepare the precursor. The precursor was calcined at different temperatures at air atmosphere for 2 h, respectively. Nanocrystalline Ni_{0.7}Mn_{0.3}Gd_xFe_{2-x}O₄ ferrites powders with different crystallite sizes were synthesized.

The structure and the crystallite sizes are tested by X-ray diffractometer (XRD) in the 2θ range 25–65° using Cu K_α radiation (λ = 0.15405 nm). The type of X-ray diffractometer is SHIMADZU Co. Tokyo Japan. The database of the Joint Committee on Powder Diffraction Data was

*Author to whom all correspondence should be addressed.

0022-2461 © 2006 Springer Science + Business Media, Inc.

DOI: 10.1007/s10853-005-1545-3

used for the interpretation of XRD spectra. The crystallite sizes are calculated using Scherrer's relationship $D = k\lambda/(w - w_1)\cos\theta$, where D is the average diameter in nm, k is the shape factor, w and w_1 are the half intensity width of the relevant diffraction peak and instrumental broadening, respectively. λ is the X-ray wavelength and θ is the Bragg's diffraction angle. The crystallite sizes of the samples are estimated from the line width of the (311) XRD peaks. Mössbauer spectrum was recorded at 295 K by a computerized Oxford MS-500 Mössbauer spectrometer of the electromechanical type in constant acceleration mode. A ^{57}Co source in a Rhodium matrix was used in a continuously distributed hyperfine magnetic field. A $25\ \mu\text{m}$ thick high purity alpha iron foil was used for calibration. The experimental data was analyzed with a standard least square fitting program assuming Lorentzian line shapes. Magnetic measurements were carried out at room temperature using a vibrating sample magnetometer (VSM) (Digital Measurement System JDM-13) with a maximum magnetic field of 10000 Oe.

3. Results and discussion

The XRD patterns of $\text{Ni}_{0.7}\text{Mn}_{0.3}\text{Gd}_{0.1}\text{Fe}_{1.9}\text{O}_4$ ferrite nanocrystals synthesized at different temperatures are shown in Fig. 1. The peaks in the spectra indicate the single-phase spinel ferrite with no extra reflections. Similar XRD patterns were observed for the other samples. The peaks become sharper with the increase in heat treatment temperatures. This indicates that the crystallite sizes are increased with the sintering temperatures.

The crystallite size of $\text{Ni}_{0.7}\text{Mn}_{0.3}\text{Gd}_x\text{Fe}_{2-x}\text{O}_4$ ferrite nanocrystals varied with the heat treatment temperatures and Gd-doped contents are listed in Table I. It can be got easily that the crystallite sizes are decreased when Gd ions were doped into Ni-Mn ferrites. And the crystallite sizes are increased with the heat treatment temperatures for all the samples. Fig. 2 shows the variation of crystallite sizes with Gd-doped contents at 600, 800 and 850°C. From Fig. 2, the decreasing trend of crystallite sizes with the increasing Gd-doped contents can be observed obviously.

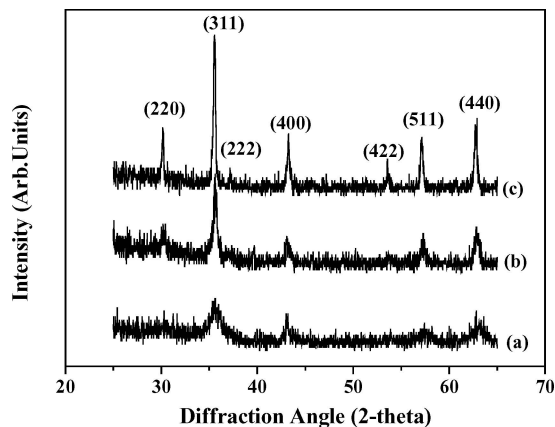


Figure 1 XRD patterns of $\text{Ni}_{0.7}\text{Mn}_{0.3}\text{Gd}_{0.1}\text{Fe}_{1.9}\text{O}_4$ ferrite nanocrystals synthesized at: (a) 600°C, (b) 800°C, and (c) 850°C.

TABLE I Crystallite sizes of $\text{Ni}_{0.7}\text{Mn}_{0.3}\text{Gd}_x\text{Fe}_{2-x}\text{O}_4$ ferrite nanocrystals varied with the heat treatment temperatures T and Gd-doped contents x

T (°C)	Crystallite sizes (nm)		
	600	800	850
$x = 0.00$	13.8	34.4	47.5
$x = 0.02$	10.3	31.7	44.8
$x = 0.04$	9.7	30.9	36.2
$x = 0.06$	10.1	23.7	38.1
$x = 0.08$	10.1	19.8	40.0
$x = 0.10$	7.8	21.0	38.6

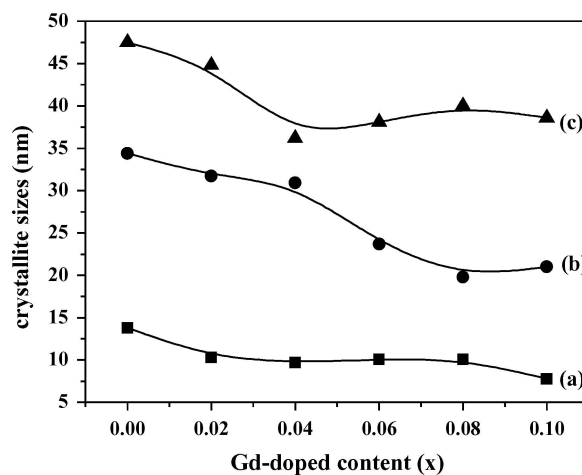


Figure 2 The crystallite sizes varied with the Gd-doped contents at: (a) 600°C, (b) 800°C, and (c) 850°C.

Such a result can be explained as follows:

The magnetic domains will be increased with the increasing heat treatment temperatures, so the crystallite sizes grow for all the samples. When some Fe ions in ferrite lattices are substituted by Gd ions, the lattice parameters will be changed [3–6]. The variation of lattice parameters will lead to the lattice strains, which produce the internal stress [5, 7, 8]. Such a stress hinders the growth of grains, so the grain sizes of the samples doped with Gd ions are smaller than that of Ni-Mn ferrite nanocrystal. On the other side, due to the larger bond energy of $\text{Gd}^{3+}\text{-O}^{2-}$ as compared with that of $\text{Fe}^{3+}\text{-O}^{2-}$, it is obvious that more energy is needed to make Gd ions enter into lattice and form the bond of $\text{Gd}^{3+}\text{-O}^{2-}$. All doped- Gd^{3+} ferrites have higher thermal stability relative to Ni-Mn ferrite nanocrystal, and hence more energy is needed for the substituted samples to complete crystallization and grains grow. Further more, some Gd ions may reside at grain boundary when Gd ions are doped into Ni-Mn ferrite [6], as the ionic radii of the Gd^{3+} ions are larger than that of Fe^{3+} ions. The presence of Gd ions at the boundary of grain will bring pressure to bear on the grains and hinder the growth of grains.

The magnetic hysteresis curves for $\text{Ni}_{0.7}\text{Mn}_{0.3}\text{Gd}_x\text{Fe}_{2-x}\text{O}_4$ ferrite nanocrystals calcined at 600°C are given in Fig. 3. It can be seen that $\text{Ni}_{0.7}\text{Mn}_{0.3}$

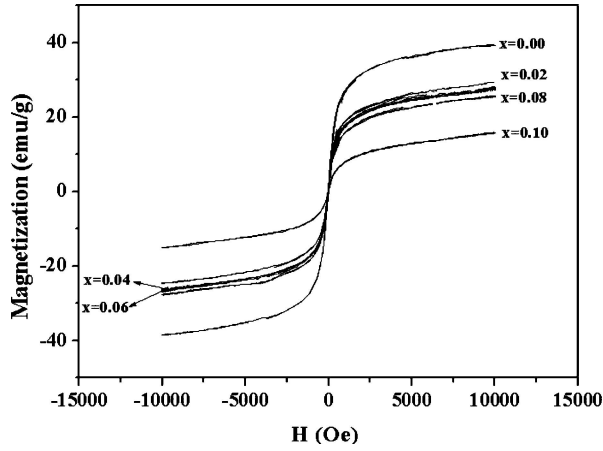


Figure 3 The magnetic hysteresis curves for $\text{Ni}_{0.7}\text{Mn}_{0.3}\text{Gd}_x\text{Fe}_{2-x}\text{O}_4$ ferrite nanocrystals calcined at 600°C with the different Gd-doped contents x .

$\text{Gd}_x\text{Fe}_{2-x}\text{O}_4$ ferrite nanoparticles only show magnetic curves without hysteresis loops, as a result, the H_c and M_r values of the samples listed in Table II are all zero. The $\text{Ni}_{0.7}\text{Mn}_{0.3}\text{Gd}_x\text{Fe}_{2-x}\text{O}_4$ ferrite nanocrystals calcined at 600°C with the crystallite sizes of 13.8, 10.3, 9.7, 10.1, 10.1 and 7.8 nm have the superparamagnetic phase corresponding to the Gd-doped content $x = 0, 0.02, 0.04, 0.06, 0.08$ and 0.10 , respectively. This can be further proved by the result of Mössbauer spectrum. The saturation magnetizations for the samples doped with Gd ions are lower than that of un-doped one and decreased with the Gd-doped contents.

Effects of Gd-doped contents and nanoparticles sizes on the magnetic properties are listed in Table II. It can be seen from Table II that the saturation magnetization values of all the samples decrease with the decreasing crystallite sizes. This may be deduced that the magnetic do-

TABLE II Effects of Gd-doped contents and nanoparticles sizes on the magnetic properties

x	T ($^\circ\text{C}$)	D (nm)	M_s (emu/g)	H_c (Oe)	M_r (emu/g)
0	600	13.8	39.5	0	0
	800	34.4	50.3	76.9	3.2
	850	47.5	55.6	47.6	2.8
0.02	600	10.3	28.9	0	0
	800	31.7	49.8	50.2	3.0
	850	44.8	53.3	46.7	2.6
0.04	600	9.7	27.9	0	0
	800	30.9	49.5	49.4	2.6
	850	36.2	53.0	46.7	2.4
0.06	600	10.1	27.8	0	0
	800	23.7	45.0	52.2	2.7
	850	38.1	52.3	41.2	2.6
0.08	600	10.1	25.6	0	0
	800	19.8	41.8	39.4	2.5
	850	40.0	48.7	47.6	2.9
0.10	600	7.8	16	0	0
	800	21.0	40.2	30	1.2
	850	38.6	48.2	54.6	3.1

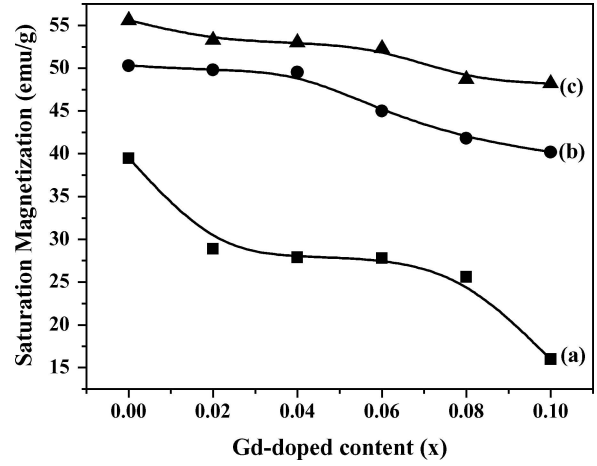


Figure 4 The saturation magnetization varied with Gd-doped contents calcined at (a) 600°C , (b) 800°C , and (c) 850°C .

mains of the nanoparticles are increased with the growth of crystallite sizes. In addition, the M_s values are decreased with the increase of Gd-doped contents at the same heat treatment temperature. Fig. 4 shows the saturation magnetization varied with the Gd-doped contents at different sintering temperatures. It can be seen clearly that the saturation magnetizations are decreased with the Gd-doped contents at the same calcination temperature, and the descending trend is becoming more and more manifest with the decrease of calcination temperatures. When calcined at 600°C , the saturation magnetization M_s of $\text{Ni}_{0.7}\text{Mn}_{0.3}\text{Gd}_x\text{Fe}_{2-x}\text{O}_4$ ferrite nanocrystals with $x = 0.0$ and 1.0 are 39.5 and 16 emu/g, respectively which particle size are 13.8 and 7.8 nm. The effects of infinite sizes may be dominant at 600°C . Change in the magnetic structure on the particles surface is significant, due to large surface/volume ratios of the nanoparticles [9]. The M_s values of Gd-doped samples are close to the un-doped sample at 800 and 850°C . When the crystallite sizes are about 30–40 nm, the samples have the similar M_s values. This may be for the following facts. The magnetic moment of Gd ions is $7.94 \mu_B$, and Gd is the only rare-earth element that the Curie temperature T_c (293.2 K) is close to room temperature. When the Fe ions are substituted by Gd ions at lattice sites, the R-R interactions are stronger than Fe-Fe interactions, so the saturation magnetization may be increased significantly. But the Gd-doped contents are less than 10% of Fe contents, the micro-substitution is not enough to increase the saturation magnetization significantly. The R-R interactions are negligible and the R-Fe interactions are weak. Especially, when the Gd-doped contents x are larger than 0.06, the M_s values are decreased slightly as compared with the other samples at the similar crystallite sizes. When the contents of doped Gd ions are increased, the doped Gd ions can't enter into the ferrite lattice totally, as the ionic radii of the Gd^{3+} ions are larger than that of Fe^{3+} ions. Hence the Fe-Fe interactions are decreased due to the reduction in the concentration of Fe ions on the B sites. All the explanations are based on the

assumption that the rare-earth ions occupy the B sites [8, 10].

From the values of coercivity H_c and remanent magnetization (M_r) listed in Table II, it can be observed that both the values of the samples calcined at 600°C are just all zero because of the existence of superparamagnetic phase. In addition, H_c and M_r values of the samples calcined at 800°C are larger than that of samples calcined at 850°C, when the Gd-doped contents are less than 0.08. This may be due to the following discussions. It's known that the magnetic anisotropy field in ferrites results mainly from the presence of Fe^{2+} ions [11]. For Gd-doped samples the concentration of Fe^{2+} ions is expected to decrease, i.e., the magnetic anisotropy decreases. Moreover, the concentration of Fe^{2+} ions is also decreased with the increasing heat treatment temperatures. When the Gd-doped contents are $x = 0.08$ and $x = 0.10$, the different result is got that the H_c and M_r values of the samples are increased with the calcinations temperatures. When the contents of doped Gd ions are increased, the doped Gd ions can't enter into the ferrite lattice totally, as the larger radii of Gd ions relative to Fe ions. So some Gd ions may reside at grain boundary and form oxide. The presence of oxide at grain boundary inhibits the motion of domain walls. The oxide will be more stable with the increasing temperatures, so the H_c values are increased with the heat treatment temperatures when the Gd-doped contents are larger than 0.06, and the maximum value of H_c for the sample calcined at 850°C is got at $x = 0.1$. However, it is shown that the coercivities values decrease with the increasing content of Gd ions when the samples are calcined at 800°C. It is due to the quite small grains with a reduced number of inner pores. Because the smaller crystallite sizes of the samples with Gd ions relative to un-doped sample, the displacement of the magnetic domain walls becomes easier and the lower coercivities are obtained.

Fig. 5 shows the Mössbauer spectra of $Ni_{0.7}Mn_{0.3}Gd_{0.1}Fe_{1.9}O_4$ ferrite nanocrystal measured at room temperatures. As evident from the Fig. 5a, the spectrum consists of a weak sextet pattern superposed on a distinct central doublet, which indicates that the sample has a ferromagnetic and superparamagnetic nature, simultaneously. A well-resolved six-line pattern of the sample with the particle sizes 21 nm is mainly attributed to the ferromagnetic behaviour in Fig. 5b. The change of magnetic phase for the ferrite powder can be explained with the variation of particle sizes as a function of annealing temperatures.

Mössbauer parameters of $Ni_{0.7}Mn_{0.3}Gd_{0.1}Fe_{1.9}O_4$ ferrite nanocrystals with the crystallite sizes of 7.8 nm (a) and 21 nm (b) are listed in Table III. δ , ΔE , B and A_0 represent isomer shift, quadrupole shift, hyperfine field and fractional area of the pattern, respectively. Table III illustrates that the δ values of A-sites is less than that of B-sites. This conclusion has been proved by many literatures [12–14]. The values of ΔE indicate the degree of deviating from cubic symmetrical structure. The absolute

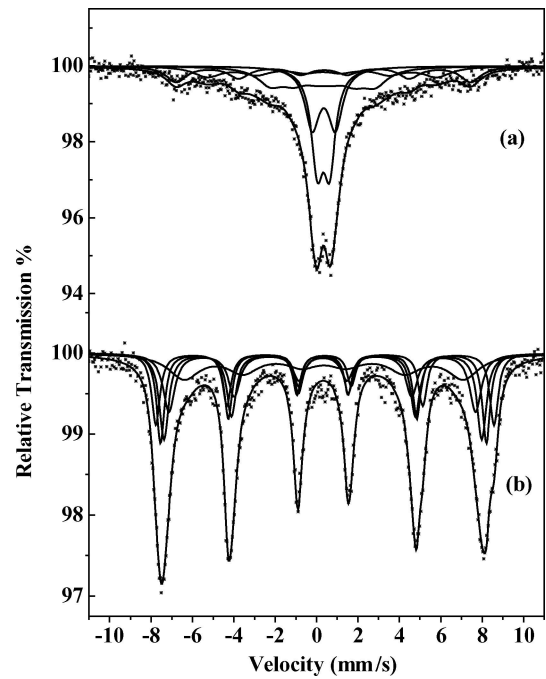


Figure 5 The Mössbauer spectrum of the $Ni_{0.7}Mn_{0.3}Gd_{0.1}Fe_{1.9}O_4$ ferrite nanocrystals with the particle sizes of 7.8 nm (a) and 21 nm (b) measured at 295 K.

values of ΔE will be increased with the decreasing particle sizes, and the asymmetrical electric fields surrounding the Mössbauer nucleus will be strengthened along with the decreasing particle sizes. Because the particle sizes are small, the crystallization will be incomplete. The value of B (B) is larger than that of B (A). This may result from that the magnetic properties are increased with the crystallite sizes. In addition, the superparamagnetism in sample (A) also make the decrease of the hyperfine field. The value of hyperfine field at B-sites B (B_1) is larger than that of at A-sites B (A_1). This may be due to the stronger A-O-B superinteraction at B-sites.

From the percent of the absorption area of the Mössbauer spectra, we can decide the cation distribution. The fraction of Fe ions at the tetrahedral A and octahedral B sites were determined using the area of Mössbauer spectra. For stoichiometric ferrite it is easy to estimate the cation distribution, but it becomes rather difficult for

TABLE III The Mössbauer parameters for $Ni_{0.7}Mn_{0.3}Gd_{0.1}Fe_{1.9}O_4$ ferrite nanocrystal with the crystallite sizes of 7.8 nm (A) and 21 nm (B)

Sample	Sublattice	δ (mm s ⁻¹)	ΔE (mm s ⁻¹)	B (kOe)	A_0
A	A ₁	0.32	0.04	343.9	0.15
	B ₁	0.38	0.04	441.3	0.17
	B ₂	0.37	0.06	157.2	0.22
	C _A	0.37	0.59	–	0.26
	C _B	0.39	1.12	–	0.20
B	A ₁	0.35	–0.04	488.2	0.20
	A ₂	0.33	0.04	459.5	0.19
	B ₁	0.43	–0.003	506.8	0.17
	B ₂	0.39	0.01	418.5	0.22
	B ₃	0.35	0.03	476.2	0.22
Error		±0.02	±0.02	±1.0	±0.02

mixed ferrites, since they contain mixtures of more than one cation other than iron. In addition, all doped-Gd ions can't enter into ferrite lattice at B sites. It is difficult to decide the amount of substituting Gd ions for Fe ions, so the cation distribution of $\text{Ni}_{0.7}\text{Mn}_{0.3}\text{Gd}_{0.1}\text{Fe}_{1.9}\text{O}_4$ ferrite nanocrystal can't be determined only by Mössbauer spectrum.

4. Conclusions

The XRD patterns show that nanocrystalline $\text{Ni}_{0.7}\text{Mn}_{0.3}\text{Gd}_x\text{Fe}_{2-x}\text{O}_4$ ferrites have single spinel structure. The crystallite sizes are decreased when Gd ions were doped into Ni-Mn ferrites. And the crystallite sizes are increased with the heat treatment temperatures for all the samples. When the crystallite sizes are about 30–40 nm, the samples have the similar M_s values. When Gd-doped contents x is larger than 0.06, all doped Gd ions can't enter into the ferrite lattice but reside at grain boundary. The maximum content of Gd^{3+} ions doped in ferrite lattices substituted by are $x = 0.06$. The values of H_c and M_r are zero for all the samples calcined at 600°C. In addition, the H_c and M_r values of the samples calcined at 800°C are larger than that of sintered at 850°C, when the Gd-doped contents are less than 0.08. When the Gd-doped contents are $x = 0.08$ and $x = 0.10$, the different result is got that the H_c and M_r values of the samples are increased with the calcinations temperatures. And all Gd-doped ions can't enter into the ferrite lattice. The experimental results of Mössbauer spectra show the ferrimagnetism of $\text{Ni}_{0.7}\text{Mn}_{0.3}\text{Gd}_{0.1}\text{Fe}_{1.9}\text{O}_4$ ferrite nanocrystal have not disappeared completely, even if the crystallite size is 7.8 nm. When the crystallite size is 21 nm, $\text{Ni}_{0.7}\text{Mn}_{0.3}\text{Gd}_{0.1}\text{Fe}_{1.9}\text{O}_4$ ferrite nanocrystal has only ferrimagnetism.

Acknowledgements

This work is supported by National Natural Science Foundation of china (NSFC) (Grant No 50372025 and 50572033).

References

1. J. SMIT and H. P. J. WIJN, "Ferrites" (Wiley, New York, 1959).
2. C. W. CHEN, "Magnetism and Metallurgy of Soft Magnetic Materials" (North-Holland, Amsterdam, 1990) p. 395.
3. N. REZLESCU, E. REZLESCU, C. PASNICU and M. L. CRAUS, *J. Magn. Magn. Mater.* **136** (1994) 319.
4. N. REZLESCU, E. REZLESCU, P. D. POPA and L. REZLESCU, *J. Alloy. Comp.* **275–277** (1998) 657.
5. A. A. SATTAR, A. H. WAFIK, K. M. EL-SHOKROFY and M. M. EL-TABBY, *Phys. Stat. Sol. (A)* **171** (1999) 563.
6. A. A. SATAR, A. M. SAMY, R. S. EL-EZZA and A. E. EATAH, *ibid.* **193**(1) (2002) 86.
7. HUA YANG, ZICHEN WANG, LIZHU SONG, MUYU ZHAO, JIANPING WANG and HELIE LUO, *J. Phys. D: Appl. Phys.* **29** (1996) 2574.
8. HUA YANG, LIJUN ZHAO, XUWEI YANG, LIANCHUN SHEN, LIANXIANG YU, WEI SUN, YU YAN, WENQUAN WANG and SHOUHUN FENG, *J. Magn. Magn. Mater.* **271** (2004) 230.
9. K. HANEDA, *Can. J. Phys.* **65** (1987) 1233.
10. N. REZLESCU, E. REZLESCU, C. PASNICU and M. L. CRAUS, *J. Phys.: Condens. Matter* **6** (1994) 5707.
11. E. W. GORTER, *Philips Res. Rep.* **9** (1954) 295.
12. H. TANG, Y. W. DU, Z. Q. QIU and J. C. WALKER, *J. Appl. Phys.* **63** (1998) 4105.
13. KWANG PYO CHAE, WON KI KIM, SUNG HO LEE and YOUNG BAE LEE, *J. Magn. Magn. Mater.* **232** (2001) 133.
14. XINYONG LI and CHARLES KUTAL, *J. Allo. Comp.* **349** (2003) 264.

Received 11 February
and accepted 18 April 2005